Supplemental Tables and Figures

Myeloperoxidase, paraoxonase-1 and HDL form a functional ternary complex

Ying Huang[1], Zhiping Wu[1,#], Meliana Riwanto[2,3], Shengqiang Gao[1], Bruce S. Levison[1], Xiaodong Gu[1], Xiaoming Fu[1], Matthew A. Wagner[1], Christian Besler[2,3], Gary Gerstenecker[4], Renliang Zhang[1], Xin-Min Li[1], Anthony J. DiDonato[1,5], Valentin Gogonea[1,4], W.H. Wilson Tang[1,6], Jonathan D. Smith[1,6] , Edward F. Plow[6,7], Paul L. Fox[1], Diana M. Shih[8], Aldons J. Lusis[8], Edward A. Fisher[9], Joseph A. DiDonato[1], Ulf Landmesser[2,3], and Stanley L. Hazen[1,6]

[1] Department of Cellular and Molecular Medicine, Center for Cardiovascular Diagnostics & Prevention
[2] Cardiology, Cardiovascular Center, University Hospital Zurich, and
[3] Cardiovascular Research, Institute of Physiology, and Center for Integrative Human Physiology, University of Zurich, Zurich, Switzerland.
[4] Department of Chemistry, Cleveland State University, Cleveland, OH 44115
[5] Department of Psychology, John Carroll University, University Heights, Ohio 44118
[6] Department of Cardiovascular Medicine, Cleveland Clinic, Cleveland, Ohio 44195, USA
[7] Department of Molecular Cardiology, Cleveland Clinic, Cleveland, Ohio 44195, USA
[8] Department of Medicine/Division of Cardiology, BH-307 Center for the Health Sciences, University of California Los Angeles, Los Angeles, CA 90095
[9] Department of Medicine, New York University, New York, New York.

[#] Current address, St Jude Children's Research Hospital, Memphis, TN 38105

Correspondence should be addressed to:
Stanley L. Hazen, Cleveland Clinic, Mail Code NC10, 9500 Euclid Avenue, Cleveland, OH 44195
Phone: (216) 444-9353; Fax: (216) 444-9404; Email: hazens@ccf.org

Supplemental Table 1

Case : Control Cohort 1 **Characteristics of the study population**

Characteristics	Healthy subjects n = 26	Acute Coronary Syndrome n = 26	p value
Demographics			
Age, mean (years)	59 ± 14	62 ± 17	n.s.
Sex (male/female)	16/10	16/10	n.s.
MAP, mean (mm Hg)	84.0 ± 8.2	88.1 ± 12.0	n.s.
Laboratory parameters			
HgbA1C (%)	5.4 ± 0.3	6.0 ± 0.4	*P*<0.05
HDL cholesterol (mg/dL)	52 ± 18	47 ± 21	n.s.
LDL cholesterol (mg/dL)	125 ± 41	108 ± 29	*P*<0.05
Triglycerides (mg/dL)	119 ± 31	137 ± 47	*P*<0.05
hsCRP (mgl/dL)	1.9 ± 1.3	3.6 ± 3.5	n.s.
Creatinine clearance	97 ± 34	86 ± 41	n.s.
Medications			
Statins (%)	0	88	
Beta blocker (%)	0	54	
Diuretic (%)	0	19	
ACE-I / ARB (%)	0	65	
Calcium blocker (%)	0	15	
Aspirin (%)	0	100	
Clopidogrel (%)	0	35	

Abbreviations: BP, blood pressure; MAP, mean arterial pressure; HDL, high-density lipoprotein: LDL, low-density lipoprotein; hsCRP, high sensitivity C-reactive protein; ACE-I, angiotensin-converting enzyme inhibitor; ARB, angiotensin receptor blocker.

Reported P values are from unpaired 2-sided *t* test.

Supplemental Table 2

Case : Control Cohort 2	**Characteristics of the study population**		
Characteristics	Healthy subjects n = 10	Acute Coronary Syndrome n = 10	p value
Demographics			
Age, mean (years)	56 ± 9	61 ± 7	n.s.
Sex (male/female)	6/4	8/2	
MAP, mean (mm Hg)	85.6 ± 7.4	91.9 ± 9.9	n.s.
Laboratory parameters			
HbA1C (%)	5.7 ± 0.2	5.9 ± 0.4	n.s
HDL cholesterol (mmol/l)	1.9 ± 0.5	1.7 ± 1.3	n.s.
LDL cholesterol (mmol/l)	2.9 ± 0.5	2.7 ± 1.0	n.s
Triglycerides (mmol/l)	1.1 ± 0.7	1.1 ± 0.4	n.s
CRP (μmol/l)	2.0 ± 1.0	3.0 ± 5.0	n.s.
Creatinine (μmol/l)	77.7 ± 8.7	75.4 ± 14.5	n.s.
Medications			
Statins (%)	0	90	
Beta blocker (%)	0	50	
Diuretics (%)	0	10	
ACE-I / ARB (%)	0	70	
Calcium blocker (%)	0	0	
Aspirin (%)	0	100	
Clopidogrel (%)	0	90	

Abbreviations: BP, blood pressure; MAP, mean arterial pressure; HDL, high-density lipoprotein: LDL, low-density lipoprotein; hsCRP, high sensitivity C-reactive protein; ACE-I, angiotensin-converting enzyme inhibitor; ARB, angiotensin receptor blocker.

Reported P values are from unpaired 2-sided *t* test.

Supplemental Figure 1

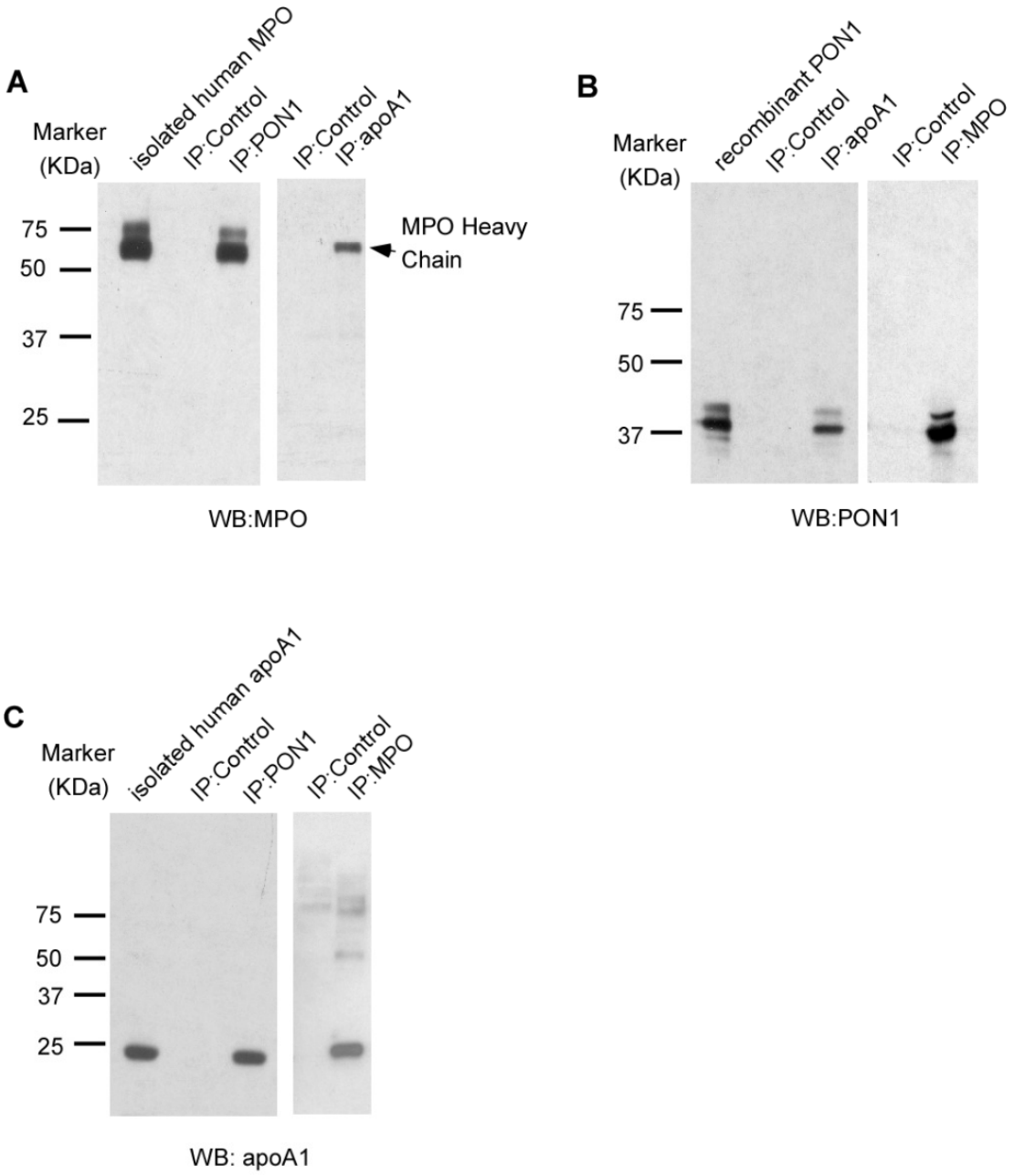

Supplemental Figure 1. Immuno-precipitation studies detected a potential complex formed between HDL, MPO and PON1 in plasma. Immunoprecipitated proteins, using specific antibodies as indicated were separated on reducing 12% SDS-PAGE gels and proteins transferred to membranes for western blot probing. (**A**) PON1 and apoA1 immunoprecipitation (IP) from plasma, followed by anti-MPO Western blot (WB). (**B**) ApoA1 and MPO IP from plasma, followed by anti-PON1 Western blot (WB). (**C**) PON1 and MPO IP from plasma followed by anti-apoA1 Western blot (WB). Primary antibodies used for detecting apoA1, MPO and PON1 were in-house mouse mAb anti-apoA1 antibody 10G1.5 (1:20,000), rabbit anti-MPO antibody (Abcam ab 76100; 1:2000) and rabbit anti-PON1 antibody (EPITOMICS, 2835-1; 1:10,000) respectively. Isolated human MPO, isolated human apoA1 and recombinant PON1 were used as positive control for all the western blots.

Supplemental Figure 2

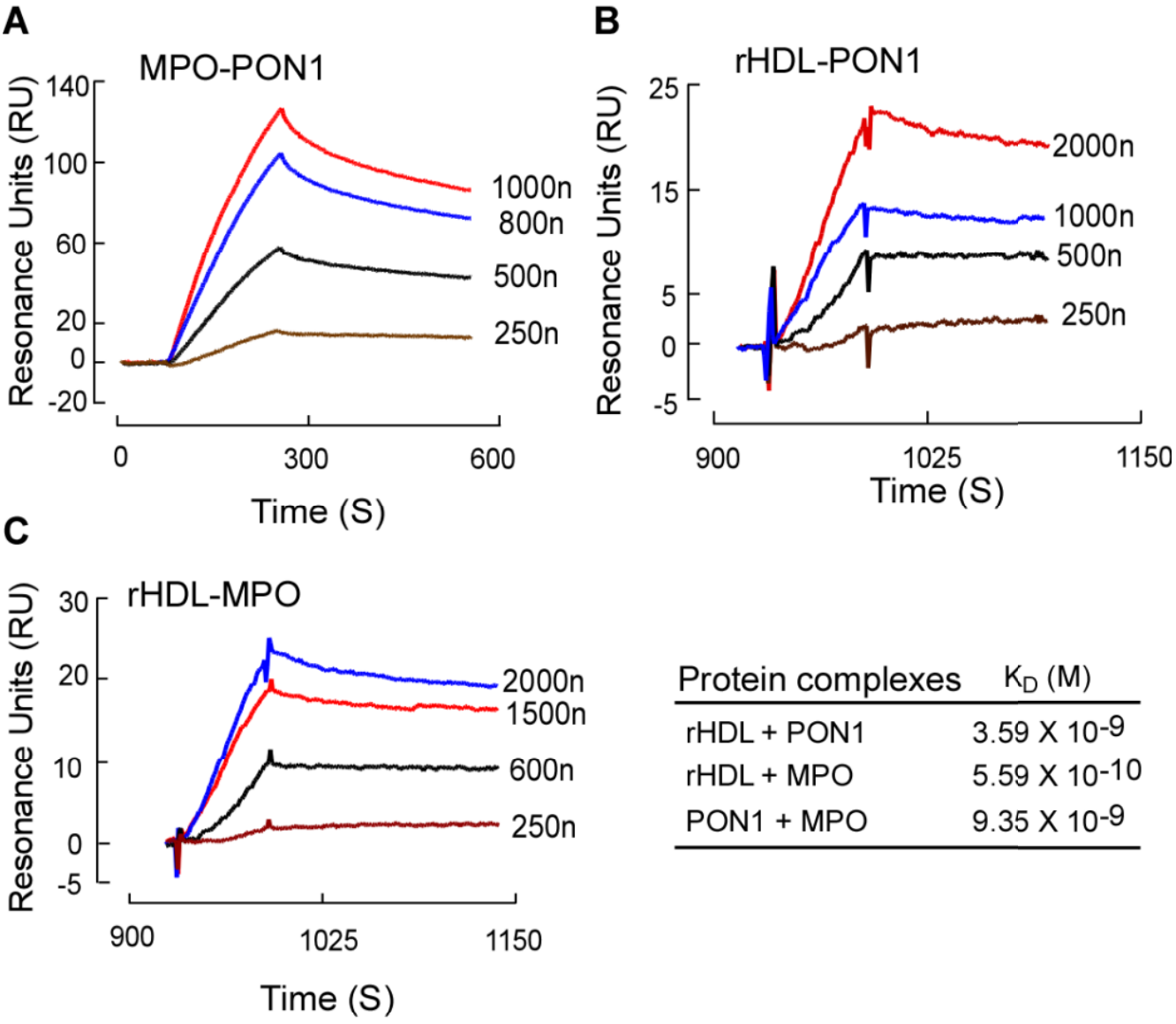

Protein complexes	K_D (M)
rHDL + PON1	3.59×10^{-9}
rHDL + MPO	5.59×10^{-10}
PON1 + MPO	9.35×10^{-9}

Supplemental Figure 2. SPR sensorgrams of rHDL, MPO and PON1 using a BIAcore 2000 system. Either MPO or nHDL were ligands bound to the sensor chip as described in "Method". Signals from a control flow cell and from buffer runs have been subtracted. (**A**) SRP sensorgrams of MPO and PON1. The concentration of analyte (PON1) is shown at the right of the sensorgram. (**B**) SPR sensorgrams of rHDL with PON1 as analyte. (**C**) SRP sensorgrams of rHDL with MPO as analyte. The K_D values are averages of three independent experiments.

Supplemental Figure 3

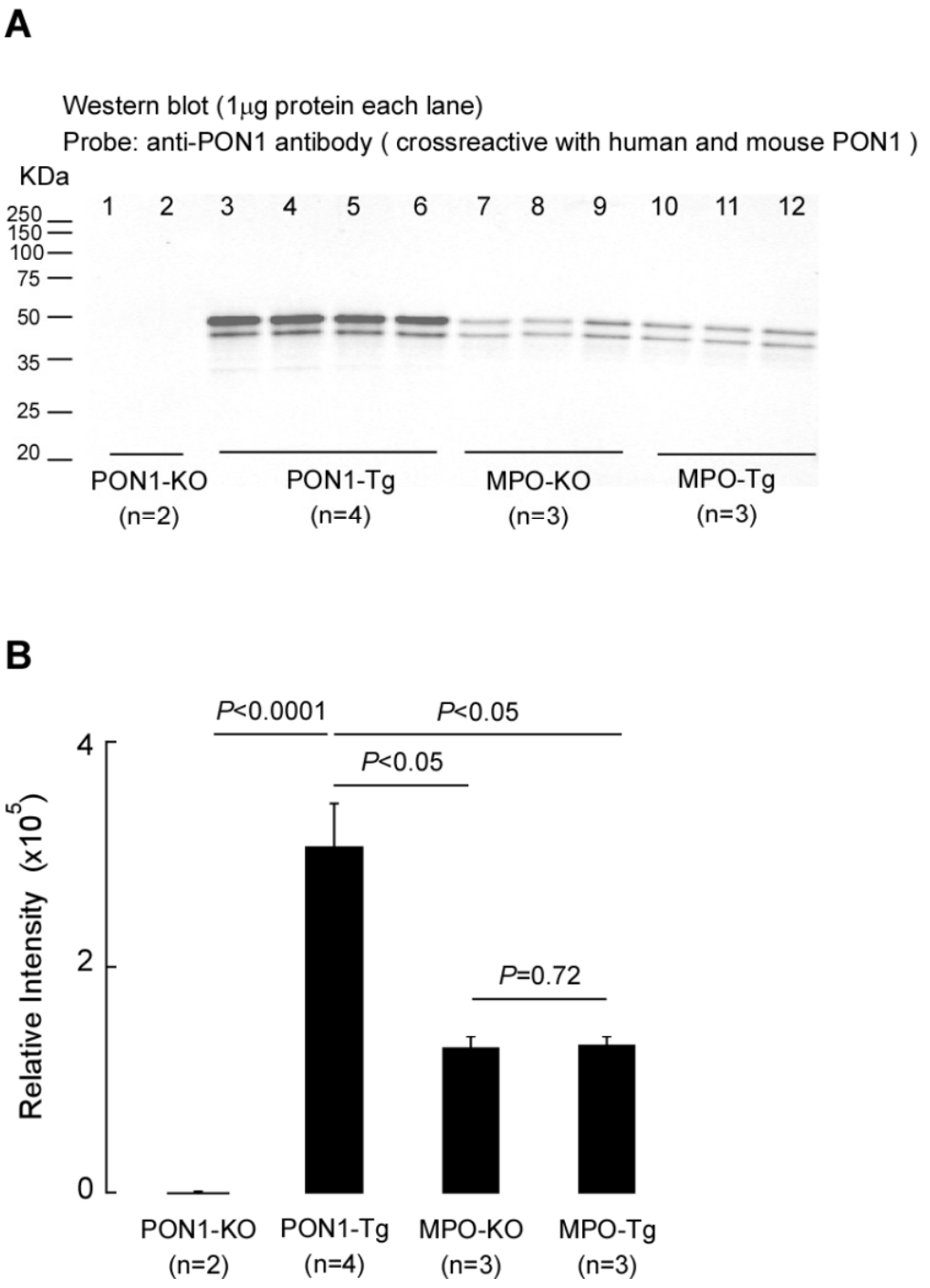

Supplemental Figure 3. PON1 abundance in mouse plasma. (**A**) Mouse plasma from mice of the indicated genotype was fractionated on a reducing 12% SDS-PAGE gel and the proteins transferred to PVDF membrane. The blot was blocked in 5% non-fat milk and incubated with anti-mouse & human PON1 antibody (1:10,000, Epitomics, Inc, cat: 2835-1) at room temperature for 1h. Primary anti-PON1 antibody was detected by IR-dye 800CW labeled anti-rabbit IgG- secondary antibody (1:10,000, LI-COR) at room temperature for 1h. (**B**) Total western blot signals were quantified by Image Studio version 2 (LI-COR) and are shown in panel B. Data shown represents mean ± SD of the indicated samples.

Supplemental Figure 4

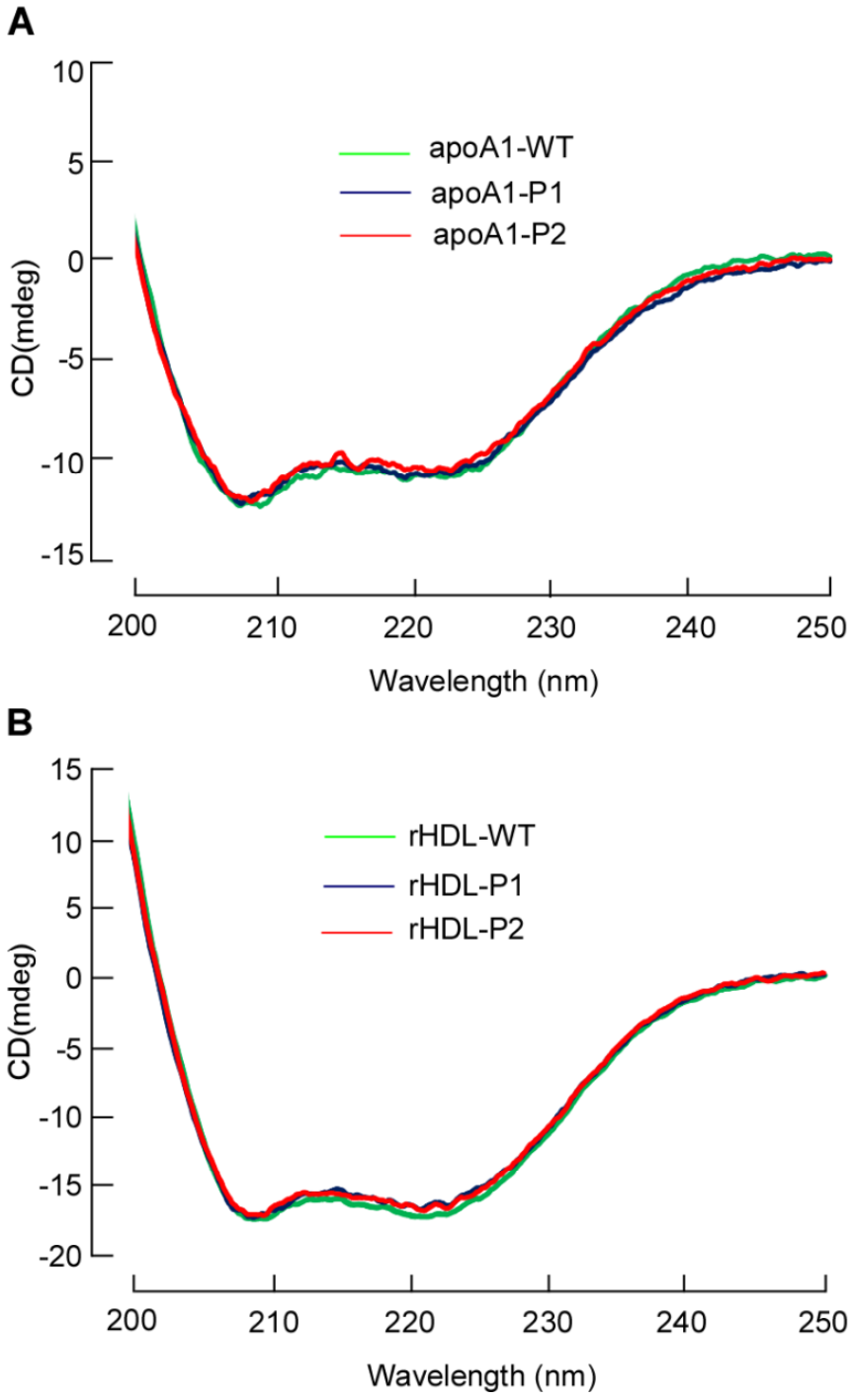

Supplemental Figure 4. CD spectral analysis of apoA1 and rHDL. (**A**) apoA1 (WT, P1 and P2 mutants, 100μg/ml) in 10mM phosphate buffer, pH 7.0. (**B**) rHDL particles made with wild type apoA1 (rHDL-WT) or the indicated different apoA1 mutants rHDL-P1 and rHDL-P2 (apoA1 100μg/ml) in 10mM phosphate buffer, pH 7.0.

Supplemental Figure 5

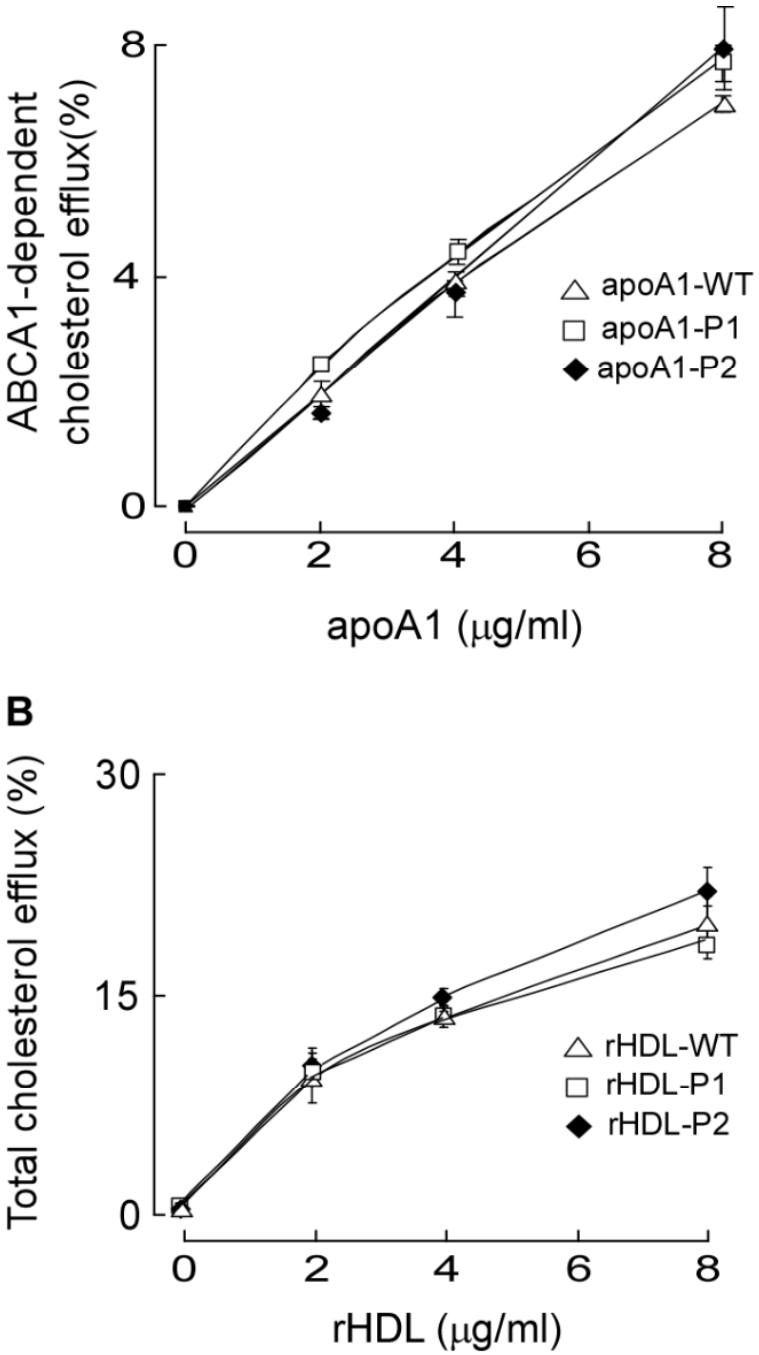

Supplemental Figure 5. Cholesterol efflux is unaffected with mutant apoA1's. ApoA1 or rHDL mediated cholesterol efflux from RAW264.7 cells indicated that wild type apoA1, P1 and P2 mutant proteins exhibited comparable cholesterol efflux activity either in their lipid-free or in their rHDL lipidated form. Indicated amounts of various apoA1's (**A**) or rHDL's (**B**) were incubated with cholesterol-loaded macrophage RAW264.7 cells in the presence or absence of 8-Br-cAMP pretreatment, and ABCA1-dependent cholesterol efflux and total cholesterol efflux were quantified as described in "Methods". rHDL-WT was rHDL produced using recombinant human apoA-I; rHDL-P1 was rHDL produced using recombinant human apoA-I mutant containing the mutant P1 peptide sequence L_{38}GEALALEL$_{46}$ and rHDL-P2 was rHDL produced using recombinant human apoA-I mutant containing the mutant P2 peptide sequence S_{201}ALAAEAE$_{208}$.

Supplemental Figure 6

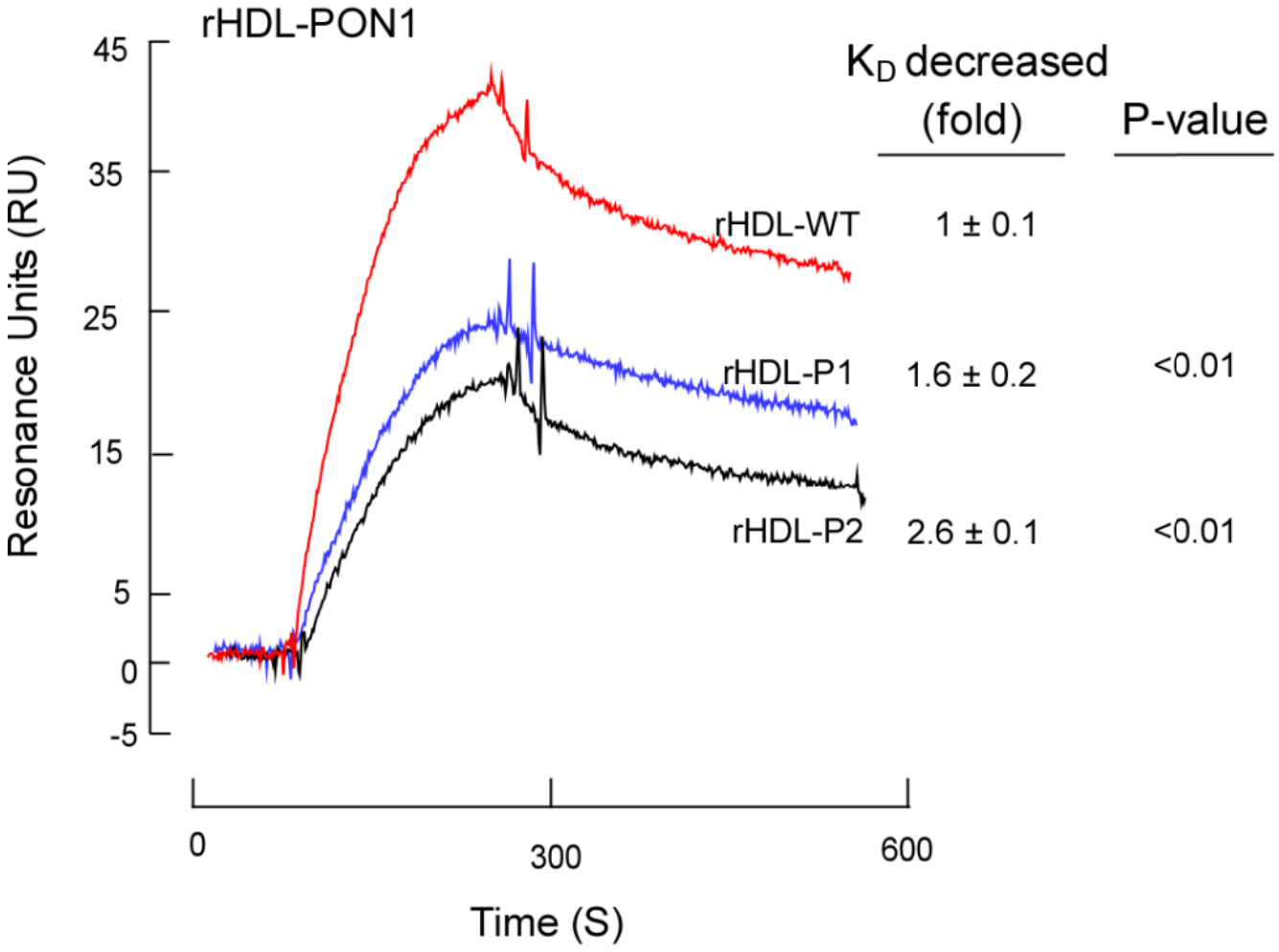

Supplemental Figure 6. Differential PON1 binding to apoA1 mutants. SPR sensorgrams of sensor chip-bound rHDL as ligand made of either wild type apoA1, P1 or P2 mutants and PON1 as analyte (400 nM) using a BIAcore 2000 system as described in "Methods". Signals from a control flow cell and from buffer runs have been subtracted. The K_D values were determined from the averages of three independent experiments and fold-decrease in K_D values relative to rHDL-WT was calculated and is shown.

Supplemental Figure 7

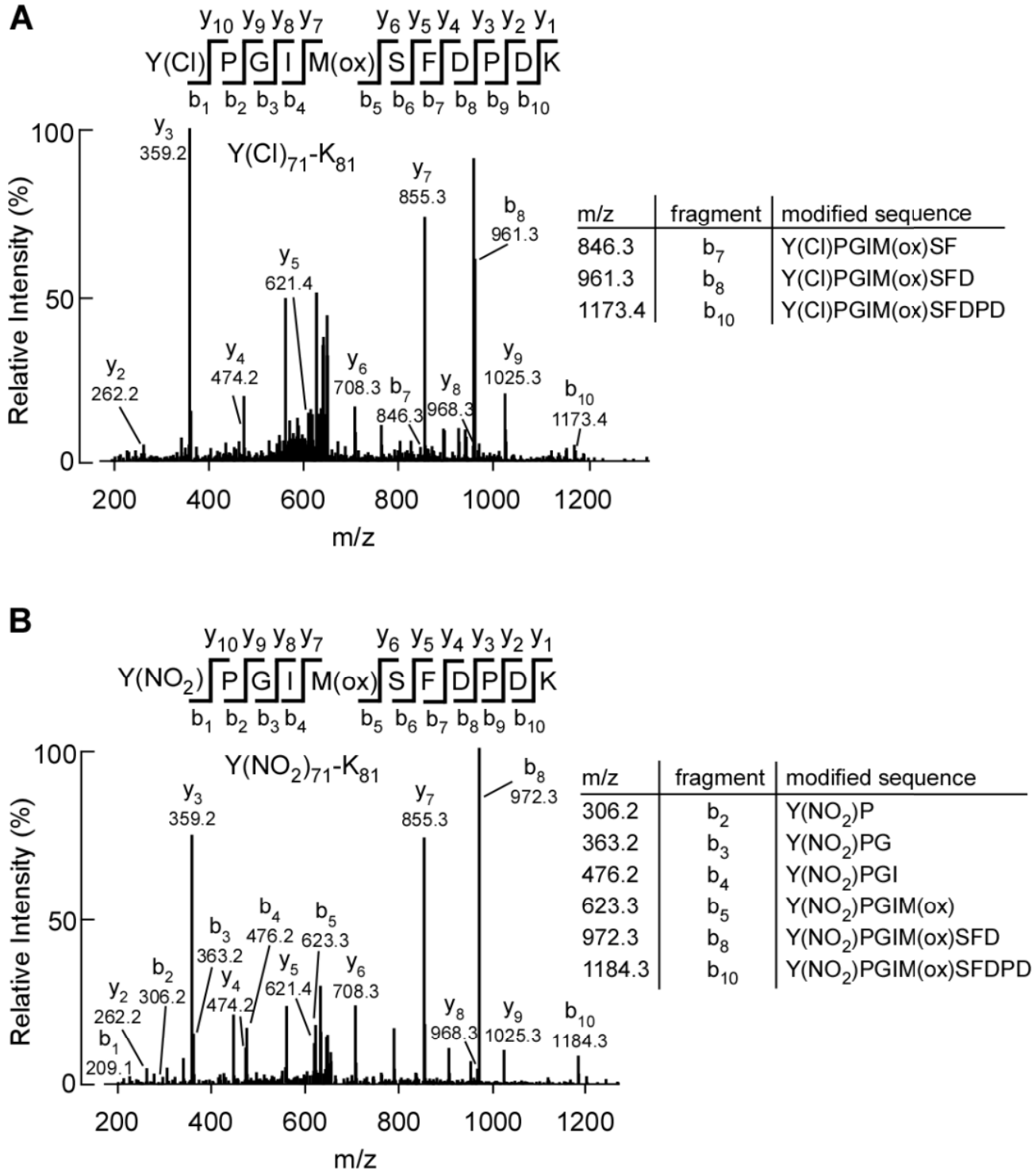

Supplemental Figure 7. CID spectra of the chlorotyrosine 71-containing peptide and the nitrotyrosine 71-containing peptide in PON1. The spectra were acquired during the analysis of in-solution tryptic digests of PON1/HDL (1:1, mol:mol) treated with either (**A**) the MPO/H_2O_2/Cl- protein chlorination system or (**B**) the MPO/ H_2O_2/NO_2 protein nitration system at 10:1 molar ratio of H_2O_2/apoA1 as described under “Methods.”

Supplemental Figure 8

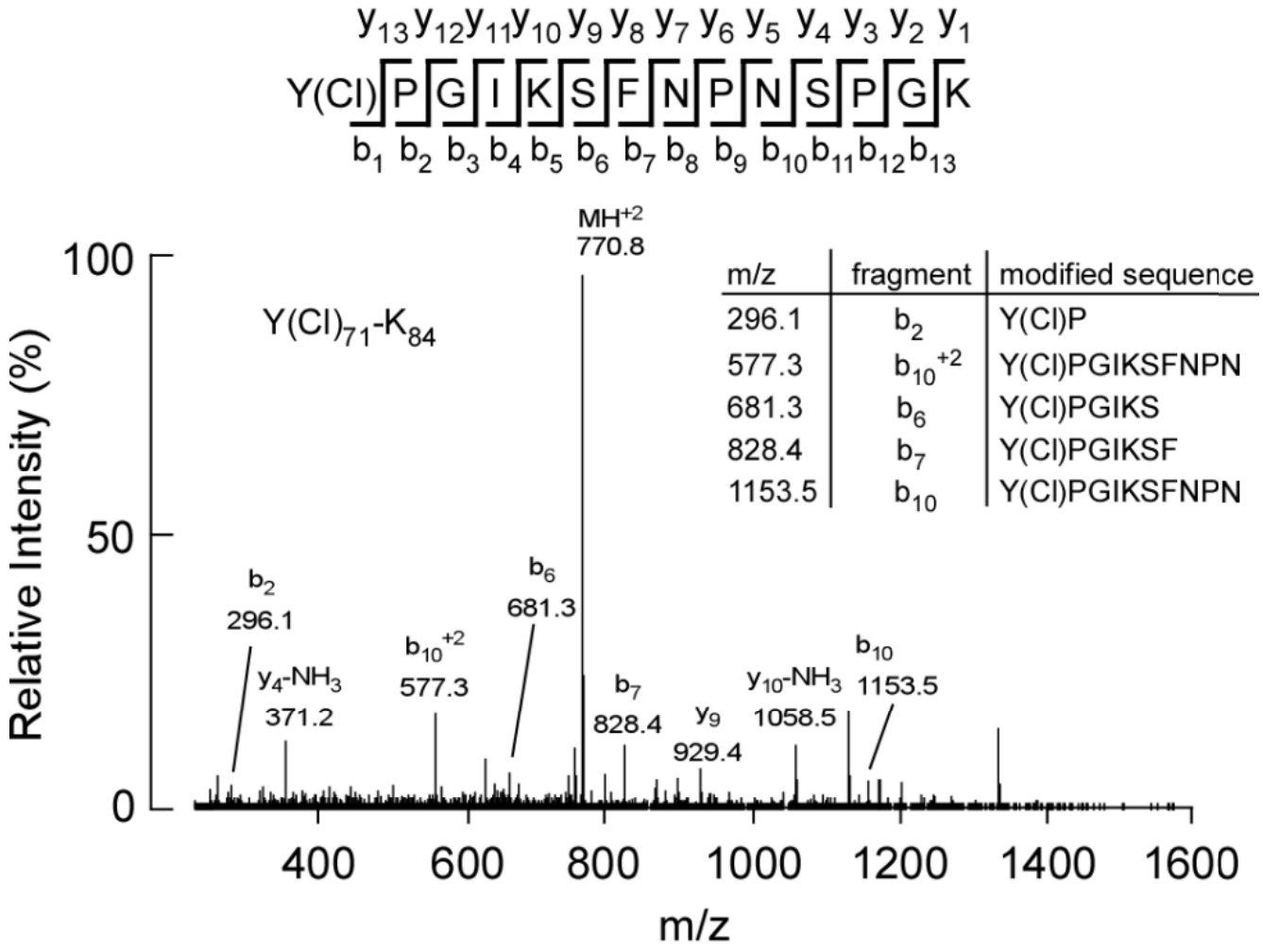

Supplemental Figure 8. Detection of chlorotyrosine 71-containing peptides in PON1 isolated from human atherosclerotic plaque by LC-tandem mass spectrometry. CID spectra were acquired after direct in-solution digestion of isolated HDL from human atherosclerotic plaque. The MS spectrum of the ^{35}Cl isotopologue for the peptide containing 3-chorotyrosine (residue 71) in PON1 is shown.

Supplemental Figure 9

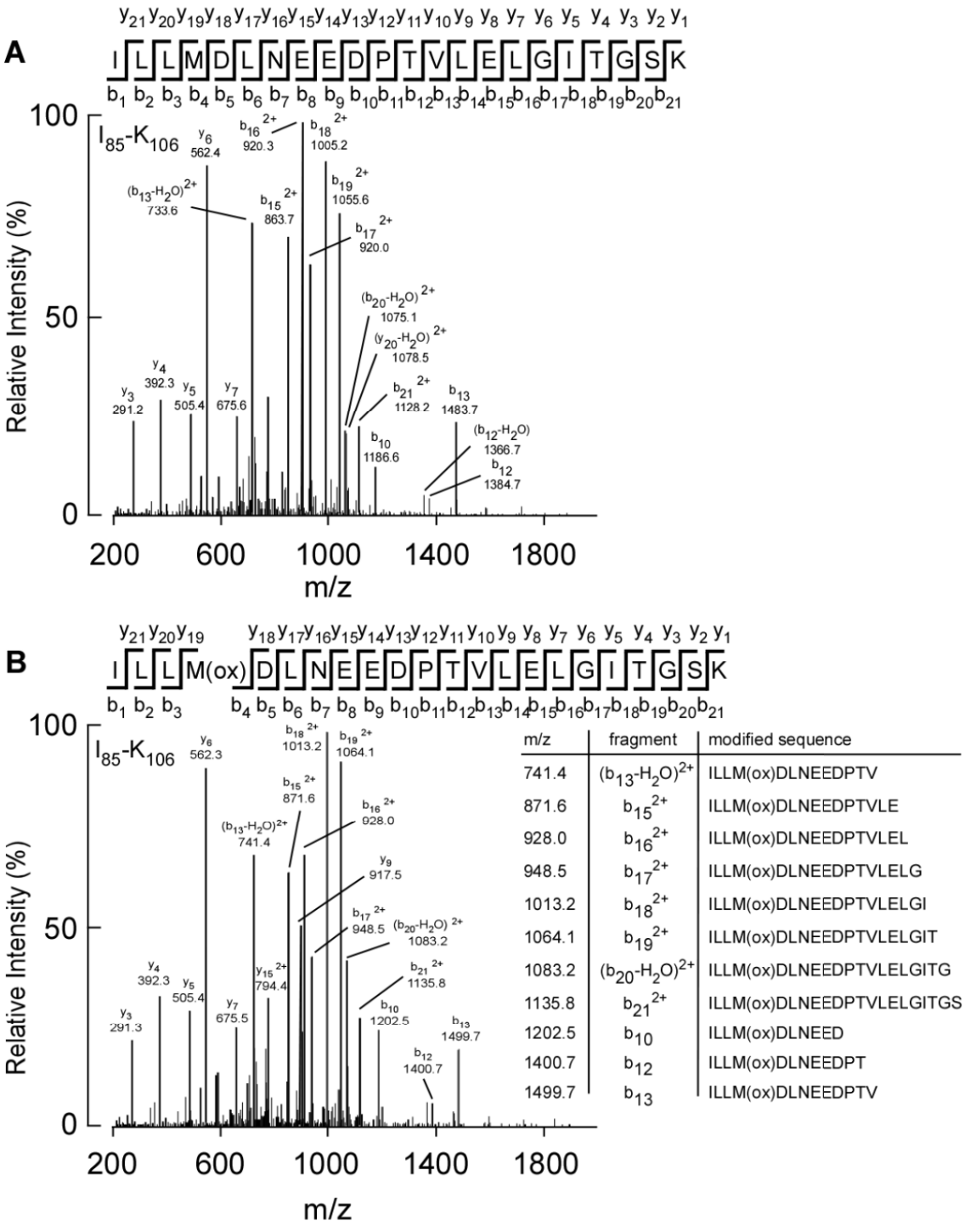

Supplemental Figure 9. CID spectra of the methionine and methionine sulfoxide containing peptides in PON1. HDL was isolated from the serum of acute coronary syndrome (ACS) and healthy non-diabetic control subjects (Case:Control cohort, Supplemental Table 2). (**A**) CID spectra of PON1 native peptide containing methionine 88. (**B**) CID spectra of PON1 peptide containing methionine sulfoxide 88.

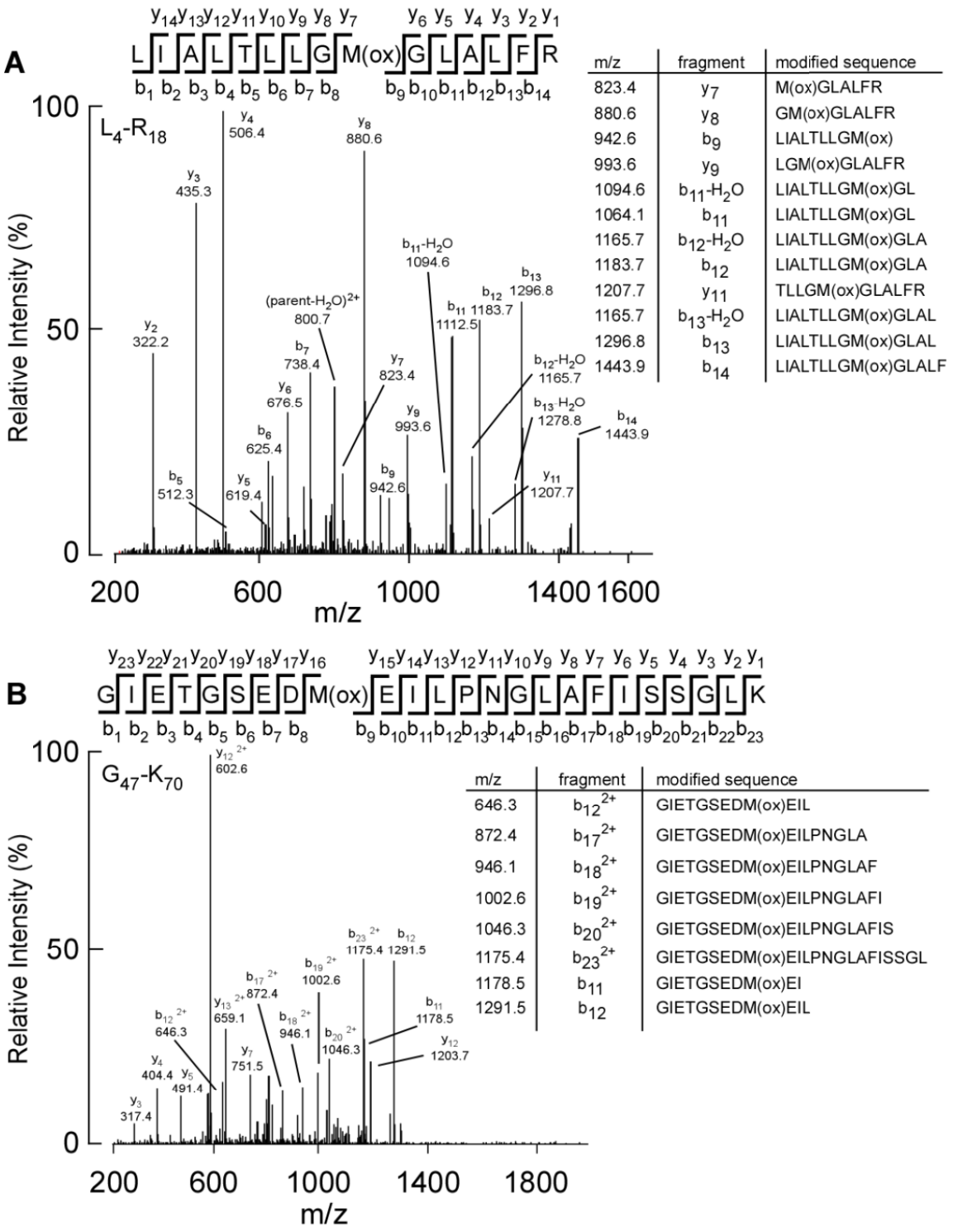

m/z	fragment	modified sequence
823.4	y_7	M(ox)GLALFR
880.6	y_8	GM(ox)GLALFR
942.6	b_9	LIALTLLGM(ox)
993.6	y_9	LGM(ox)GLALFR
1094.6	b_{11}-H_2O	LIALTLLGM(ox)GL
1064.1	b_{11}	LIALTLLGM(ox)GL
1165.7	b_{12}-H_2O	LIALTLLGM(ox)GLA
1183.7	b_{12}	LIALTLLGM(ox)GLA
1207.7	y_{11}	TLLGM(ox)GLALFR
1165.7	b_{13}-H_2O	LIALTLLGM(ox)GLAL
1296.8	b_{13}	LIALTLLGM(ox)GLAL
1443.9	b_{14}	LIALTLLGM(ox)GLALF

m/z	fragment	modified sequence
646.3	b_{12}^{2+}	GIETGSEDM(ox)EIL
872.4	b_{17}^{2+}	GIETGSEDM(ox)EILPNGLA
946.1	b_{18}^{2+}	GIETGSEDM(ox)EILPNGLAF
1002.6	b_{19}^{2+}	GIETGSEDM(ox)EILPNGLAFI
1046.3	b_{20}^{2+}	GIETGSEDM(ox)EILPNGLAFIS
1175.4	b_{23}^{2+}	GIETGSEDM(ox)EILPNGLAFISSGL
1178.5	b_{11}	GIETGSEDM(ox)EI
1291.5	b_{12}	GIETGSEDM(ox)EIL

Supplemental Figure 10. CID spectra of the methionine sulfoxide containing peptides in PON1. HDL was isolated from the serum of acute coronary syndrome (ACS) and healthy non-diabetic control subjects (Case:Control cohort, Supplemental Table 2). (**A**) CID spectra of PON1 peptide containing methionine sulfoxide 12. (**B**) CID spectra of PON1 peptide containing methionine sulfoxide 55.

Supplemental Figure 11

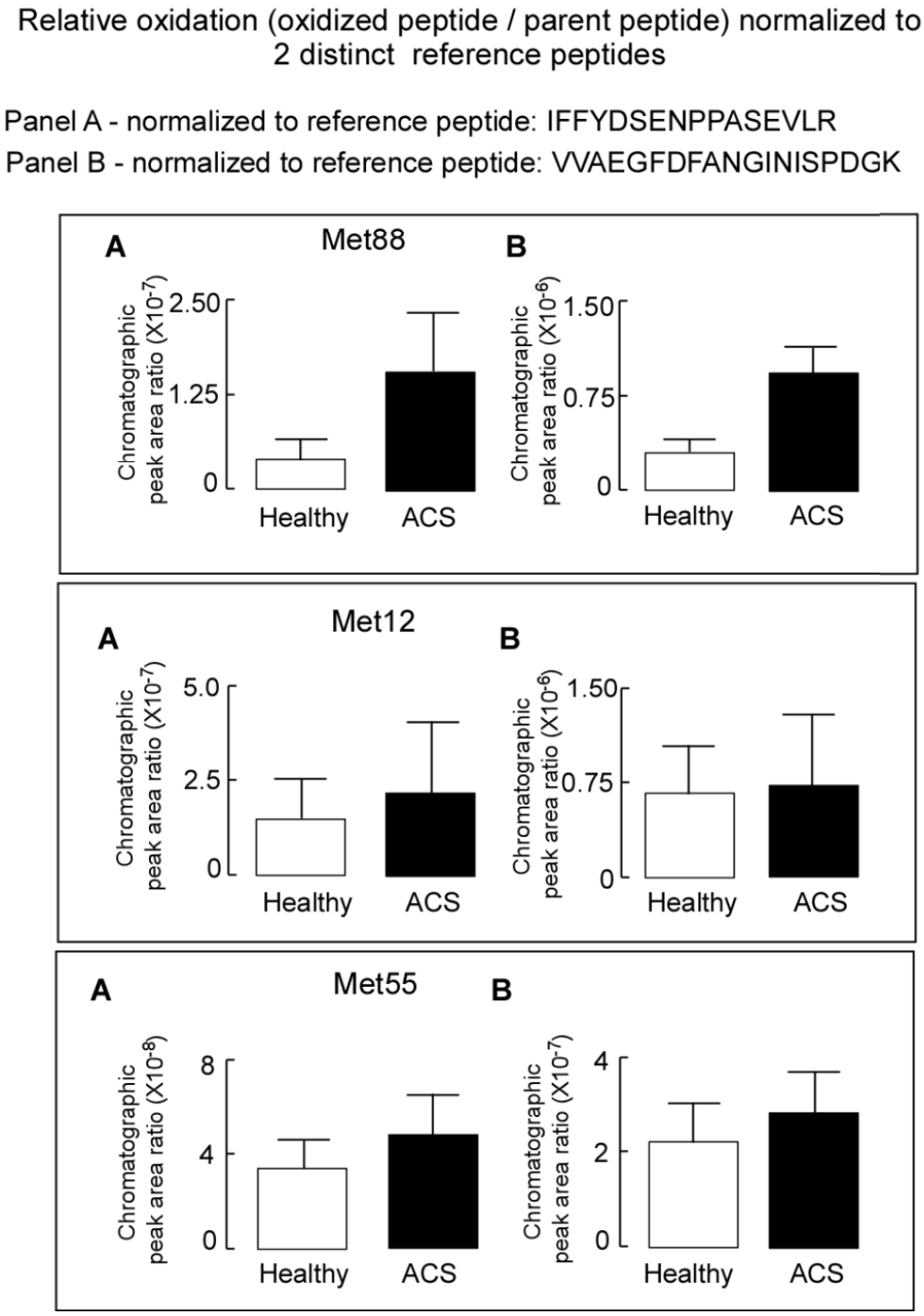

Supplemental Figure 11. PON1 is a site-specifically targeted for oxidation during acute coronary syndrome (ACS). HDL was isolated from the serum of acute coronary syndrome (ACS) and healthy non-diabetic control subjects (Case:Control cohort, Supplemental Table 2). Three methionine residues (Met88, Met55 and Met12) within PON1 were reproducibly detected and quantified. Results shown are expressed as relative oxidation (oxidized peptide/parent peptide) normalized to 2 distinct reference peptides. Panel A: peak area ration normalized to reference peptide: IFFYDSENPPASEVLR. Panel B – peak area ratio normalized to reference peptide: VVAEGFDFANGINISPDGK.

Supplemental Figure 12

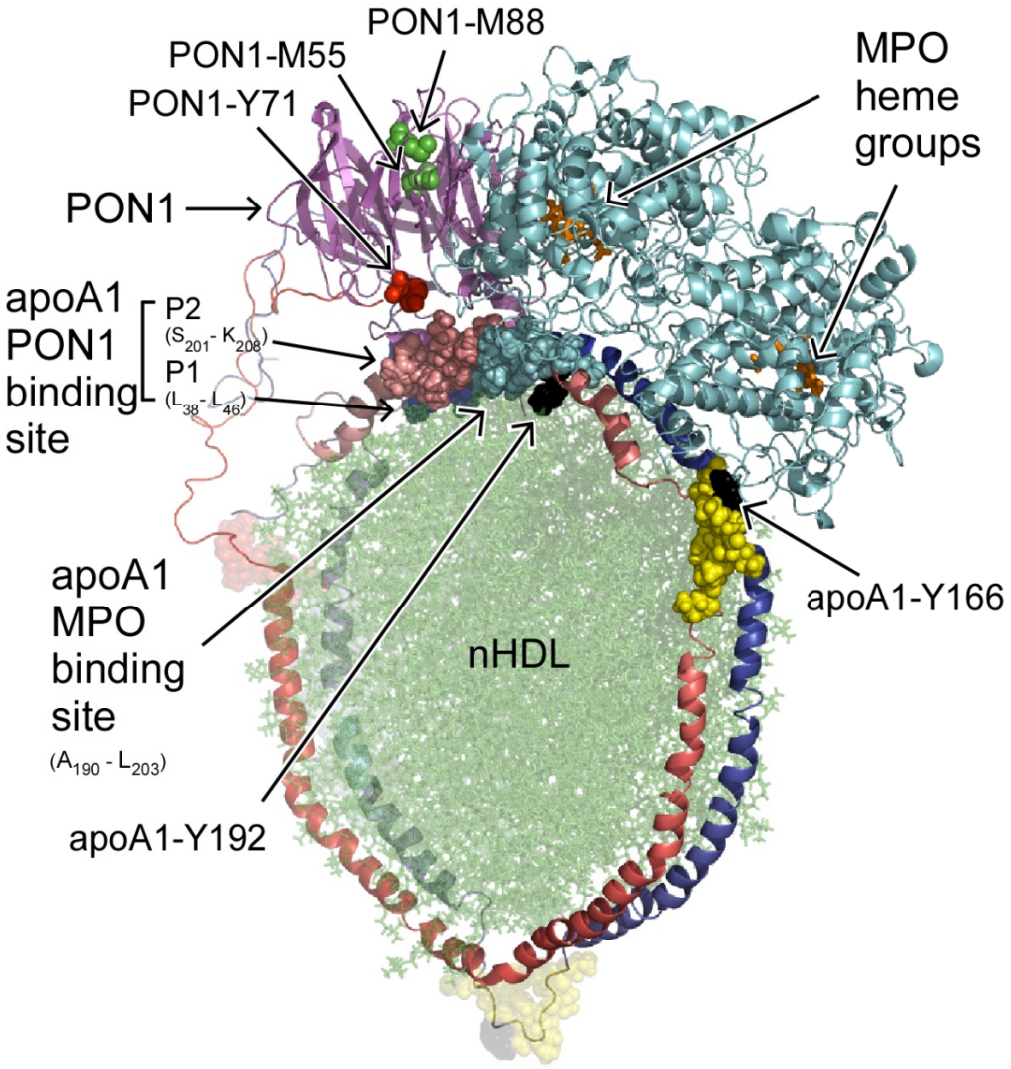

Supplemental Figure 12. Structural model of hypothetical ternary complex of MPO and PON1 bound to discoidal nHDL. The structural model of a hypothetical ternary complex of MPO and PON1 bound to discoidal nHDL, as in Figure 7, but using the all-atom solar-flares model of nascent HDL (ref. 43) as scaffolding. The two predominantly alpha helical apoAI chains in nHDL are aligned in a head to tail anti-parallel double belt arrangement, N-termini colored with dark red/blue, and C-termini colored with light red/blue. Phospholipids in the lipid core of are depicted in semitransparent green. The PON1 binding sites on apoA1 shown are P1 (L38-L46, filled blue) and P2 (S201-K208, filled light red). The adjacent MPO-binding site on apoA1 (residues A190-L203, filled light blue) is also depicted. Site-specific oxidative modifications found in PON1 recovered from isolated HDL from either atherosclerotic lesions or ACS plasma include Tyr71 (red) and Met55 and Met88 (both green). Met12 of PON is not shown because the N-terminus (16 amino acids) of PON1 was not resolved in the PON1 crystal structure reported. The location of the openings to the two heme pockets on the MPO homodimer are predicted to be in close spatial proximity to site-specific oxidative modifications reported in apoA1 recovered from human atherosclerotic plaque, Tyr166 and Tyr192 (filled black). Also shown are the "solar flare" regions of apoA1, presumed LCAT interaction sites (filled yellow).

Supplemental Figure 13

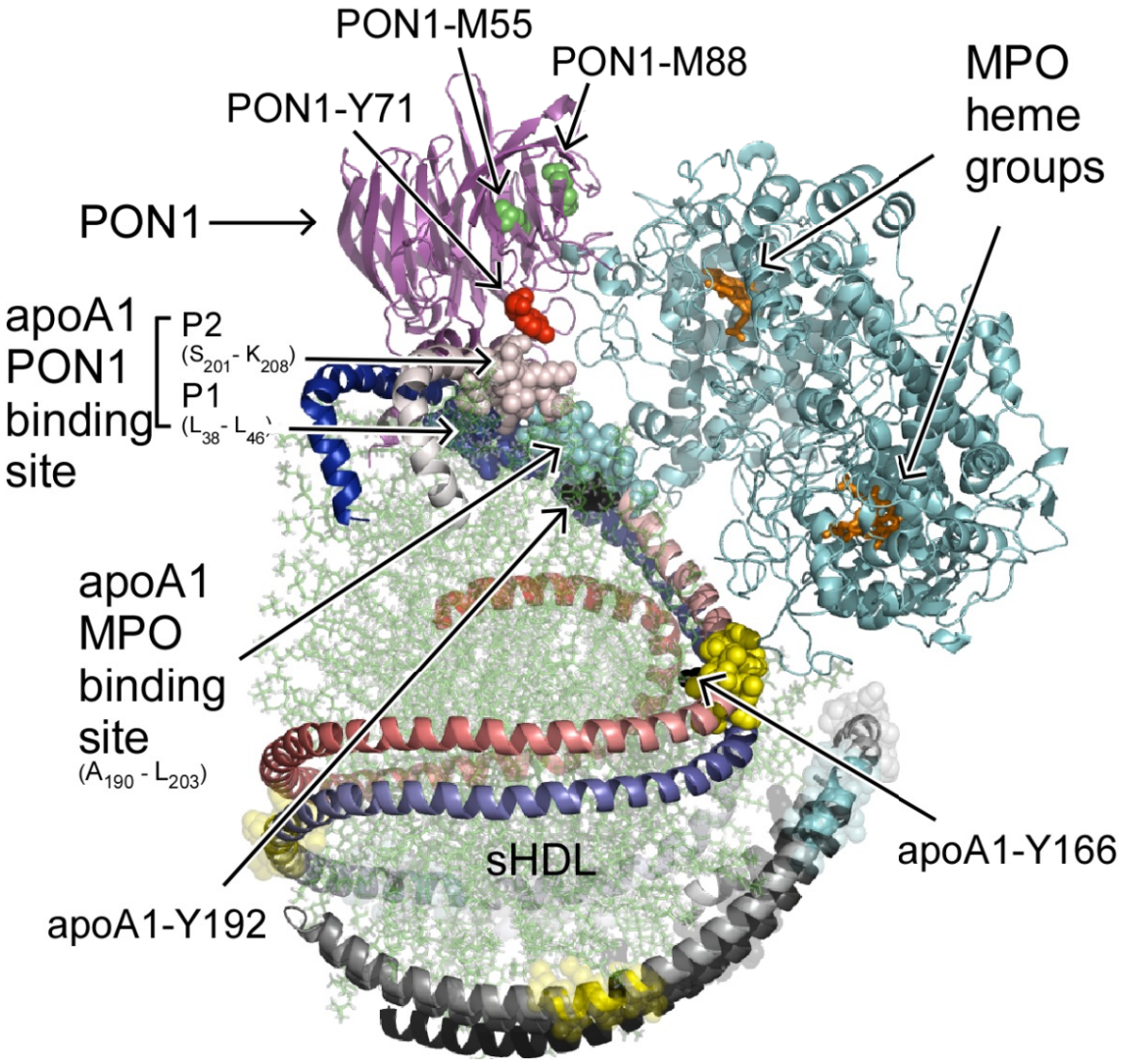

Supplemental Figure 13. Structural model of hypothetical ternary complex of MPO and PON1 bound to spherical HDL. The structural model of a hypothetical ternary complex of MPO and PON1 bound to spherical HDL, as in Figure 7, but using the all-atom Spherical HDL model (ref. 44) as scaffolding. The molecular model of the apoA1 trimer is shown as three chains (gradient-colored *red*, *blue* and *cyan),* oriented as an anti-parallel double chain dimer and a hairpin monomer. Phospholipids in the lipid core of are depicted in semi-transparent green. The PON1 binding sites on apoA1 shown are P1 (L38-L46, filled blue) and P2 (S201-K208, filled light red). The adjacent MPO-binding site on apoA1 (residues A190-L203, filled light blue) is also depicted. Site-specific oxidative modifications found in PON1 recovered from isolated HDL from either atherosclerotic lesions or ACS plasma include Tyr71 (red) and Met55 and Met88 (both green). Met12 of PON is not shown because the N-terminus (16 amino acids) of PON1 was not resolved in the PON1 crystal structure reported. The location of the openings to the two heme pockets on the MPO homodimer are predicted to be in close spatial proximity to site-specific oxidative modifications reported in apoA1 recovered from human atherosclerotic plaque, Tyr166 and Tyr192 (filled black). Also shown are the "solar flare" regions of apoA1, presumed LCAT interaction sites (filled yellow).